Park, J., Lühr, H., Michaelis, I., Stolle, C., Rauberg, J., Buchert, S., Gill, R., Merayo, J. M. G., Brauer, P. (2015):Westward tilt of low-latitude plasma blobs as observed by the Swarm constellation. - *Journal of Geophysical Research*, *120*, 4, p. 3187-3197.

DOI: http://doi.org/10.1002/2014JA020965

AGU PUBLICATIONS

JGR

Journal of Geophysical Research: Space Physics

RESEARCH ARTICLE
10.1002/2014JA020965

Key Points:
- Low-latitude plasma blobs exhibit a westward tilt on the horizontal plane
- Blobs are tilted westward on the plane perpendicular to the ambient B field
- The blob structure is field aligned

Correspondence to:
J. Park,
pj@kasi.re.kr

Citation:
Park, J., H. Lühr, I. Michaelis, C. Stolle, J. Rauberg, S. Buchert, R. Gill, J. M. G. Merayo, and P. Brauer (2015), Westward tilt of low-latitude plasma blobs as observed by the Swarm constellation, *J. Geophys. Res. Space Physics*, *120*, 3187–3197, doi:10.1002/2014JA020965.

Received 30 DEC 2014
Accepted 14 MAR 2015
Accepted article online 1 APR 2015
Published online 22 APR 2015

Westward tilt of low-latitude plasma blobs as observed by the Swarm constellation

Jaeheung Park[1], Hermann Lühr[2], Ingo Michaelis[2], Claudia Stolle[2,3], Jan Rauberg[2], Stephan Buchert[4], Reine Gill[4], Jose M. G. Merayo[5], and Peter Brauer[5]

[1]Korea Astronomy and Space Science Institute, Daejeon, Korea, [2]Helmholtz Centre Potsdam GFZ German Research Centre for Geosciences, Potsdam, Germany, [3]Faculty of Sciences, University of Postdam, Potsdam, Germany, [4]Swedish Institute of Space Physics, Uppsala, Sweden, [5]DTU Space, National Space Institute, Technical University of Denmark, Kongens Lyngby, Denmark

Abstract In this study we investigate the three-dimensional structure of low-latitude plasma blobs using multi-instrument and multisatellite observations of the Swarm constellation. During the early commissioning phase the Swarm satellites were flying at the same altitude with zonal separation of about 0.5° in geographic longitude. Electron density data from the three satellites constrain the blob morphology projected onto the horizontal plane. Magnetic field deflections around blobs, which originate from field-aligned currents near the irregularity boundaries, constrain the blob structure projected onto the plane perpendicular to the ambient magnetic field. As the two constraints are given for two noncoplanar surfaces, we can get information on the three-dimensional structure of blobs. Combined observation results suggest that blobs are contained within tilted shells of geomagnetic flux tubes, which are similar to the shell structure of equatorial plasma bubbles suggested by previous studies.

1. Introduction

Localized regions of enhanced plasma density are occasionally found in the low-latitude nighttime ionosphere, which are called plasma blobs (hereafter, "blobs"). This phenomenon was first reported by *Oya et al.* [1986] and *Watanabe and Oya* [1986] using in situ electron density measurements by Hinotori at about 600 km altitude. Until the last decade the blob was generally deemed as originating from an equatorial plasma bubble (EPB), based on their temporal/spatial proximity and similarities in power spectra and in vertical drift [*Le et al.*, 2003], similarity in ion composition and in electron temperature variation [*Park et al.*, 2003], magnetic conjugacy of blobs and EPBs [*Yokoyama et al.*, 2007], or metamorphosis of EPBs into blobs [*Martinis et al.*, 2009]. However, a number of papers published after 2010 argued that not all blobs are related to EPBs, at least around the latest deep solar minimum [*Kil et al.*, 2011; *Klenzing et al.*, 2011; *Choi et al.*, 2012; *Haaser et al.*, 2012; *Miller et al.*, 2014]. Now it is generally accepted that multiple mechanisms are responsible for creating blobs [*Huang et al.*, 2014].

It has been known that EPB structures are tilted with respect to the vertical direction. Radar observations found that EPBs exhibit a westward tilt on a vertical, near-equatorial plane (i.e., a plane approximately perpendicular to the ambient magnetic field) [*Woodman*, 2009, and references therein]. On the other hand, nightglow images on a global scale showed that EPBs appear as inverted-C structures on the horizontal plane: i.e., EPBs reaching further westward with increasing latitude [*Kelley et al.*, 2003]. Note that the equatorial and the horizontal planes are not coplanar but nearly perpendicular to each other. Putting these previous works (i.e., westward tilt on the equatorial and horizontal planes) into a three-dimensional context, *Kil et al.* [2009] explicitly suggested a tilted depletion shell model for EPB structures. Later, *Park et al.* [2009] supported the shell model by interpreting the polarization of magnetic field deflections around EPBs.

On the contrary, little is known about the three-dimensional structure of blobs. *Pimenta et al.* [2004] reported a few horizontal images of blobs obtained by a ground-based airglow camera. But no detailed discussion was given as to whether blobs are tilted eastward or westward on the horizontal plane. *Park et al.* [2010] reported two blob events of which the field-aligned current (FAC) structure could be interpreted as westward tilted current sheets. Those authors suggested that the two examples provide supporting evidences for a blob westward tilt on the plane perpendicular to the ambient magnetic field. However, further studies with clearer observational evidence are warranted for understanding blob structures in detail.

In this study we investigate the tilt of blob structures using the Swarm satellite constellation. Combining information about blob cross sections on two nonparallel planes (i.e., on the horizontal plane and on the plane perpendicular to the ambient magnetic field), we suggest a three-dimensional model of blob structures. In section 2 a brief description of the satellites and instruments is given. The observation results are given in section 3, which are discussed further in section 4. Finally, we summarize our findings and draw conclusions in section 5.

2. Instrumentation

The Swarm constellation is composed of three identical satellites, which were launched on 22 November 2013. Each satellite carries an electric field instrument (EFI), which measures ion density/temperature/velocity and electron density/temperature twice per second. A vector field magnetometer (VFM) measures the geomagnetic field vectors at a rate of 50 Hz, which are decimated to create 1 Hz magnetic field data. All the three satellites had near-circular orbits at similar altitudes (~500 km) from launch until mid-January 2014. During this period the separation between adjacent satellites was ~0.5° in geographic longitude (GLON) and ≤8° in geographic latitude (GLAT). In other words, it takes ≤ 2 min for adjacent satellites to cross the same GLAT. This period was within the Swarm commissioning phase. In this study we make use of the electron density and magnetic field data obtained from December 2013 to mid-January 2014.

The early mission phase mentioned in the preceding paragraph is a unique opportunity for investigating blob structures. First, all the Swarm satellites were at similar altitudes, from which we can deduce the horizontal structure of blobs. Second, the GLON separation of the adjacent satellites (~0.5°) is smaller than blob sizes reported previously (~1°) [*Pimenta et al.*, 2004]. Third, the along-track separation between satellites was ≤2 min in flight time, while blob lifetime reported by *Pimenta et al.* [2004, Figure 3] was at least 20 min. Hence, if all the three satellites observe blobs at similar GLAT, it is highly probable that they encountered different parts of the same blob structure.

Then, we move our focus from the horizontal plane to a plane perpendicular to the ambient magnetic field (hereafter, "perpendicular plane"). Deflections of the magnetic field on that plane can describe FAC structures related to plasma irregularities such as blobs [*Aggson et al.*, 1992; *Stolle et al.*, 2006; *Park et al.*, 2010]. Our data processing uses 1 Hz magnetic field vector data in the spacecraft coordinate system, which were obtained by coordinate transformation of the sensor frame VFM data. We first apply Savitzky-Golay low-pass filter (order = 3, window size = 71s, cutoff period ~1min) to the *B* field data. The low-pass-filtered time series serve as a proxy for the ambient magnetic field (hereafter, "mean field"). The mean field is subtracted from the original data, which leads to residuals (hereafter, "residual *B* field"), reflecting small-scale deflections of the magnetic field (spatial scale<~400 km). Finally, we transform the residual *B* field from the spacecraft coordinate system into the Mean-Field-Aligned (MFA) system: *x* (hereafter, "meridional") is toward higher McIlwain L shells, *y* (hereafter, "zonal") is toward magnetic east, and *z* (hereafter, "parallel") is along the mean field. We apply the same procedure to calculate residuals of magnetic field strength (*F*) measured by the Advanced Scalar Magnetometer (ASM) on board Swarm.

Blobs that we identified during the Swarm commissioning phase are typically located around 20°N in magnetic latitude (MLAT). Near that location the perpendicular plane is not horizontal but makes an angle of ~50° with the horizontal plane. Combining the two-dimensional structures in the horizontal and perpendicular planes allows us to constrain the three-dimensional structure of blobs. In this study we use the electron density data from SW_PREL_EFI files (version number 0102) and B-field data from SW_OPER_MAG files (version number 0302). Anyhow, different data versions are not expected to change our main conclusions because we use (1) "relative" variations of plasma density (e.g., cross-correlation analysis as shown in the following section) and (2) *B* field readings in the "sensor frame."

3. Results

Figure 1 shows a typical example of blobs observed during the Swarm commissioning phase. Figures 1 (first, second, and third panels) present latitudinal profiles of plasma density measured by Swarm C, A, and B, respectively. Figure 1 (fourth panel) shows each satellite track using the same color as for plasma density. Each cross mark on the track represents integer minutes in universal time (UT), and triangles are added every 10 min. Note that the order of Figures 1 (first, second, and third panels) (Swarm C/A/B) corresponds to that of magnetic longitude (MLON) of each satellite track. All three satellites encountered blobs around 20°MLAT, which exhibit

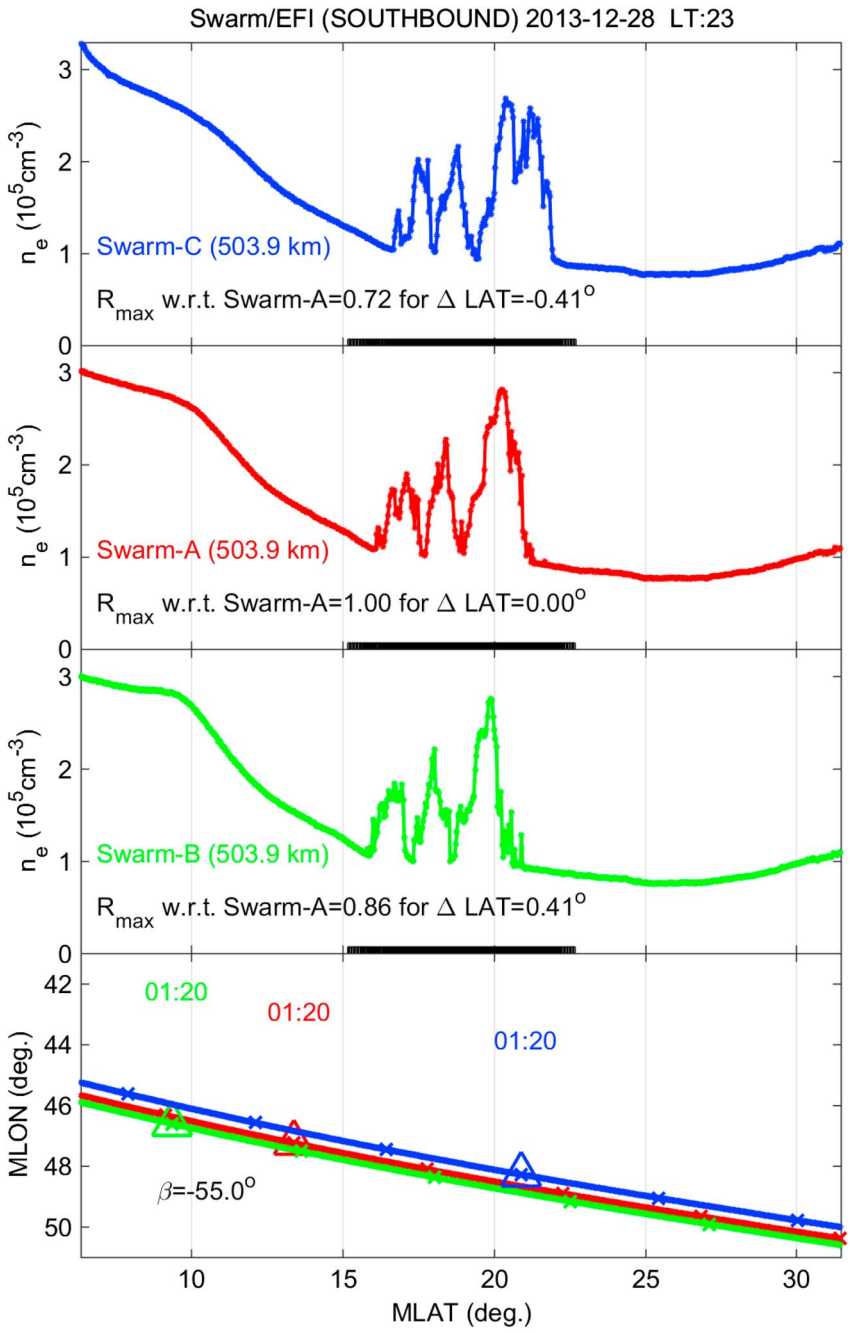

Figure 1. A typical example of blobs observed during the Swarm commissioning phase. (first, second, and third panels) Latitudinal profiles of plasma density measured by Swarm C, A, and B, respectively. (fourth panel) Each satellite track using the same color as for plasma density. Each cross mark on the track represents integer minutes in UT, and triangles are added every 10 min. R_{max} is the maximum cross-correlation coefficient between two satellites, and β is the tilt angle from magnetic east resulting from the correlation analyses.

similar morphologies among each other. By cross correlating the plasma density profiles, we can find maximum correlation coefficient (R_{max}) between the profile pairs and the optimal offset in MLAT, both of which are listed in Figures 1 (first, second, and third panels). R_{max} values are quite high (>0.7), implying that the three satellites observed one blob structure. Blobs observed by the most western Swarm C (eastern Swarm B) satellite are at highest (lowest) MLAT. That is, the blobs are extended from magnetic northwest to southeast in the Northern Hemisphere. Combining the optimal MLAT offset with MLON difference between the most eastern and western satellites (hereafter, Method A), we can approximately estimate the average angle between

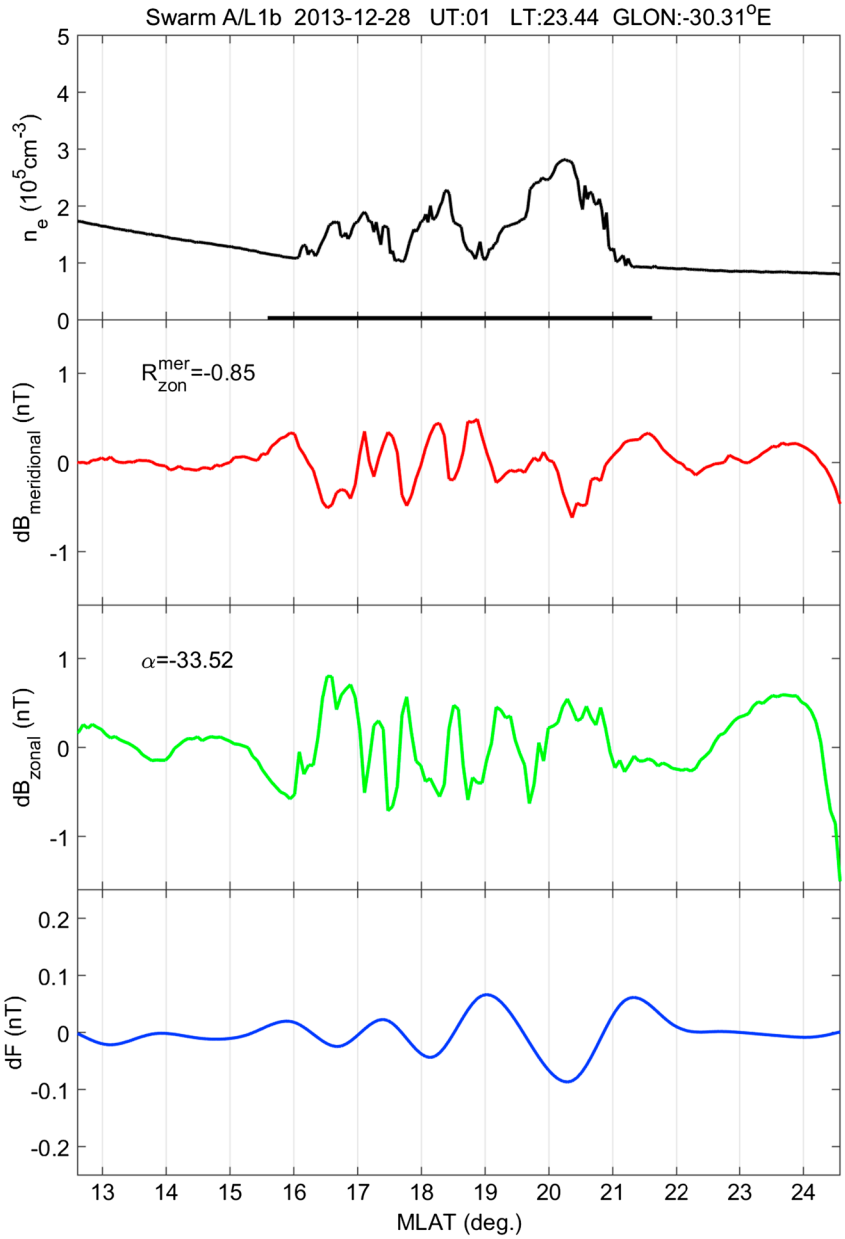

Figure 2. Variations of the residual *B* field around the blobs shown in Figure 1. (first row) The plasma density profiles shown in Figure 1. (second and third rows) Meridional and zonal components of the residual *B* field, respectively. (fourth row) Residuals of magnetic field strength.

the blob structure and magnetic east (β, positive counterclockwise), which is listed in Figure 1 (fourth panel) ($\beta \sim -55°$).

Note that Swarm A data are used as a reference for the cross correlation shown in Figure 1. To show that our method of β estimation is robust, we chose Swarm C as a reference for cross correlation and recalculated the angle β. The result was $\beta \sim -54°$, which is nearly the same as the value given in Figure 1 ($\beta \sim -55°$). We also calculated β in an alternative way (hereafter, Method B). Combining the optimal "GLAT" offset with "GLON" difference between the most eastern and western satellites, we can estimate the average angle between the blob structure and "geographic" east. This angle is further corrected for the geomagnetic declination angle to yield β: the result was $\sim -52°$, which is nearly the same as deduced by the other method ($-55°$).

In estimating β, we have assumed that the Swarm observations can be combined into a snapshot image of blobs. That is, we have assumed that the time between blob encounters by different Swarm satellites

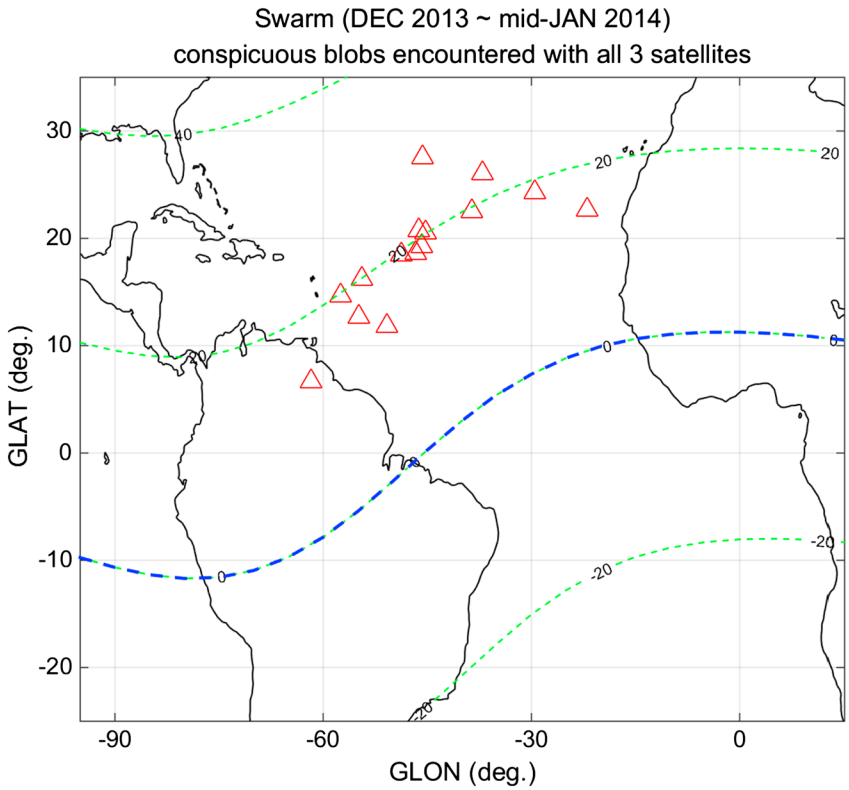

Figure 3. Global distributions of conspicuous blobs encountered near simultaneously by all the three Swarm satellites at similar locations. The dashed curves represent MLAT.

(1–3 min) is much shorter than that which is needed for significant changes in the blob morphology and/or location. The former assumption (morphological stationarity) is partially justified by the high R_{max} values shown in Figure 1. The latter assumption (positional stationarity during 1–3 min) is supported by the following arguments. In Figure 1 the total MLAT difference between blob encounters by Swarm Bravo and Swarm Charlie is about 0.82° (~90 km), and the corresponding time difference is about 3 min. If this MLAT difference were solely due to blob drift effect, the speed should be about 500 m/s, which seems to be too high for the near-midnight ionosphere. For example, the zonal drift speed of blobs is about 0.1 km/s according to *Pimenta et al.* [2004] (there has been no study on meridional speed of blobs to the best of the authors' knowledge). In conclusion, the MLAT difference in Figure 1 cannot be fully explained by blob drift effects, and therefore we invoke a horizontal tilt of blob structures.

Figure 2 shows variations of the residual *B* field around the blobs shown in Figure 1. Only Swarm Alpha data are shown as representative, but data from the other satellites (Swarm Bravo and Swarm Charlie) exhibit similar behavior. Figure 2 (first row) reproduces the plasma density profiles shown in Figure 1. Figures 2 (second and third rows) present meridional and zonal components of the residual *B* field, respectively. Figure 2 (fourth row) shows residuals of magnetic field strength, which reflects the diamagnetic effect. We can identify fluctuations in all residual *B* field components around the blobs. The correlation coefficient between the zonal and meridional residual *B* fields (R_{zon}^{mer}, within the MLAT range marked by horizontal black bars in Figure 2, first row) is listed in Figure 2 (second row.) The correlation coefficient is significantly negative, which implies that the zonal and meridional components within the blob regions pose a linear relationship, which can be represented by a slant line (hereafter, "maximum variance direction") on the perpendicular plane. The tilt angle of the maximum variance direction with respect to magnetic east (α, positive counterclockwise) is calculated and listed in Figure 2 (third row) ($\alpha = -28° \pm 5°$ on average over the three Swarm satellites).

By visual inspection of the Swarm/EFI data between December 2013 and mid-January 2014 we identified 15 cases where all the three satellites encountered conspicuous blobs at similar locations near simultaneously. Geographic locations of these 15 events are shown as triangles in Figure 3, while the dashed curves represent

Table 1. Details of the Blob Events Shown in Figure 3

Date	L T	R_{max}	β	α_{SwA}	α_{SwB}	α_{SwC}	α_{mean}	$\alpha_{calculated}$	$\alpha_{calculated} - \alpha_{mean}$
2013-12-10	01	0.96	−49	−36	−32	−(no data)	−34	−30	04
2013-12-11	01	0.87	−68	−45	−46	−48	−46	−47	−01
2013-12-12	01	0.89	−74	−48	−47	−62	−52	−63	−11
2013-12-14	01	0.91	−30	(no data)	−28	−31	−29	−18	11
2013-12-16	00	0.95	−08	(no data)	−23	−21	−22	−05	17
2013-12-18	00	0.58	55	−20	−19	−22	−20	−41	(outlier) 61
2013-12-24	00	0.90	−56	−32	−43	−42	−39	−35	03
2013-12-24	00	0.95	−52	−55	−48	−40	−48	−36	12
2013-12-24	00	0.91	−33	−30	−48	−42	−40	−25	15
2013-12-26	00	0.79	−63	−55	−46	−41	−47	−40	07
2013-12-27	00	0.81	−83	−40	−47	−54	−47	−78	−31
2013-12-28	23	0.87	−52	−34	−28	−23	−28	−35	−07
2013-12-30	23	0.66	−45	−28	−35	−25	−29	−30	−01
2014-01-01	23	0.96	−04	−29	−33	−32	−31	−03	29
2014-01-04	23	0.90	−51	−20	−43	−10	−24	−35	−11

MLAT lines. Characteristics of each blob event are detailed in Table 1. First, if we focus on the blob structures projected on the "horizontal" plane, 14 out of the 15 cases exhibit a westward tilt: i.e., blobs observed by the westernmost (easternmost) Swarm satellite are at the most poleward (equatorward) position. The average tilt angle on the horizontal plane (β in Table 1) is about −48°. The remaining one case exhibits westward (eastward) tilt between Swarm B (Swarm C) and Swarm A. However, note that the maximum cross-correlation coefficient (R_{max}) between Swarm C and Swarm A (i.e., where the blob structure appears to be tilted eastward) was only about 0.5 in this case: i.e., the two satellites may have observed different blob morphologies. We believe that the optimal latitude offsets estimated for this case are not as reliable as for the other 14 cases with westward tilt. Second, if we focus on the blob structures projected on the "perpendicular" plane, the zonal and meridional residual *B* fields are anticorrelated for all the 15 cases, with a median of the correlation coefficients of about −0.69. The average tilt angle on the perpendicular plane (α_{mean} in Table 1) is about −36°.

4. Discussion

In the following the 3-D structure of blobs is suggested from the 15 examples of blob observations described in Table 1. During the period of interest all the three Swarm satellites were close together, as already mentioned in section 2. Hence, the combined observations of plasma density can constrain the horizontal projection of a three-dimensional blob structure. For 14 out of the 15 cases mentioned in section 3, blobs observed by the westernmost (easternmost) Swarm satellite are at the most poleward (equatorward) position. These results can be interpreted as a blob structure tilted toward west: i.e., progressing westward with increasing MLAT on the horizontal plane, as shown in Figure 4a.

On the other hand, the transverse components of the residual *B* field variations can constrain the blob structure projected on the perpendicular plane. For all the 15 cases mentioned in section 3, zonal and meridional components of the residual *B* field exhibit an anticorrelation around the blobs. In the schematic diagram shown in Figure 4b, (1) blobs are accompanied by FAC sheets around the plasma irregularity walls [e.g., *Aggson et al.*, 1992; *Park et al.*, 2010]. The FACs are believed to be driven by the divergence of horizontal *F* region currents [e.g., *Aggson et al.*, 1992]. And (2) the FAC sheets are tilted westward toward increasing L shell values. The resultant residual *B* field (shown as a red arrow named "db") exhibits an anticorrelation between its zonal and meridional components, just as shown in Figure 2. Note the anticorrelation between zonal and meridional residual *B* fields holds even if the FAC direction is reversed and the arrow in Figure 4b is rotated by 180°.

As the 15 blob events in our study occurred at low latitudes (−40° < MLAT < 40°), the perpendicular plane is not parallel to the horizontal plane. To explain the westward tilt of EPBs on the two noncoplanar planes (i.e.,

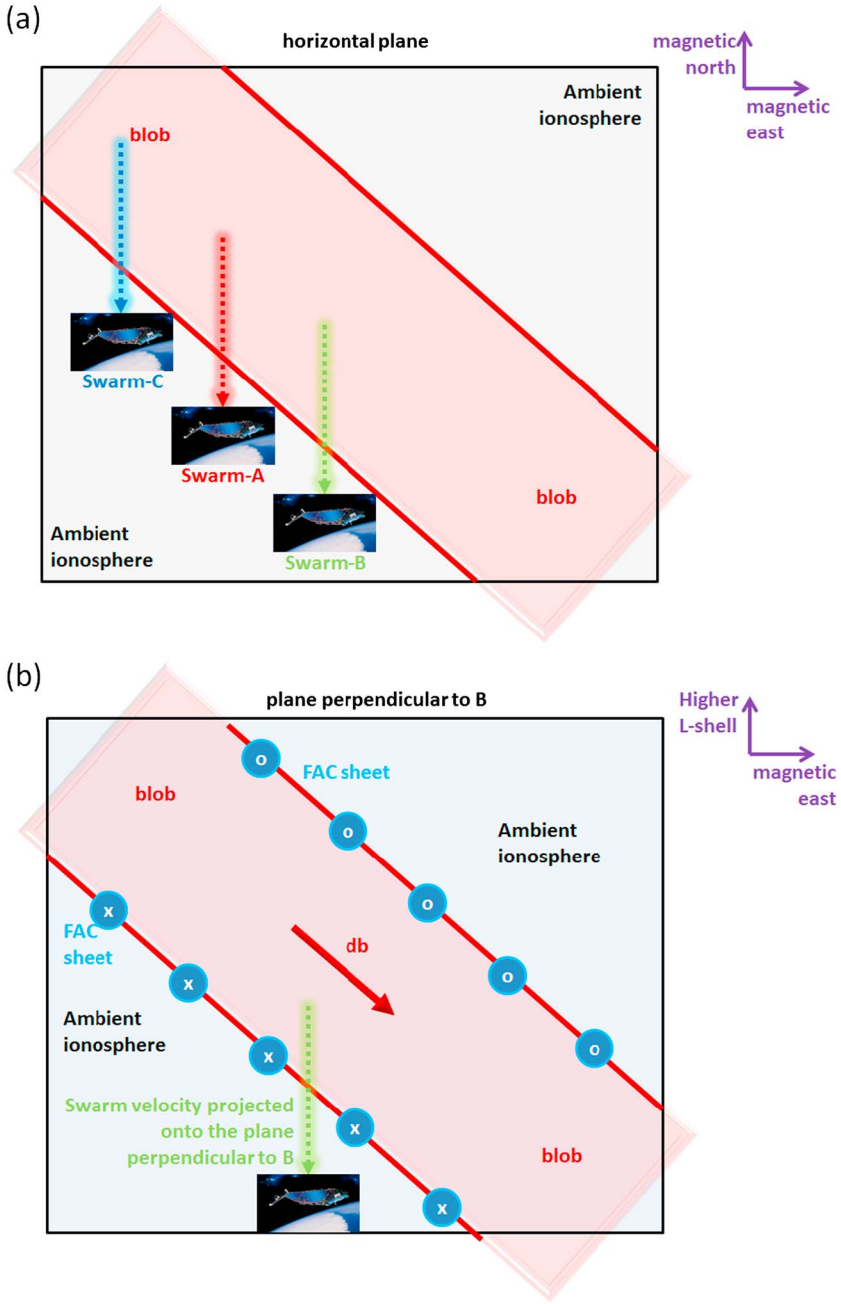

Figure 4. Schematic blob structures projected (a) on the horizontal plane and (b) on the perpendicular plane.

on the horizontal and equatorial planes), *Kil et al.* [2009] suggested that EPBs have a three-dimensional tilted shell structure [see also *Park et al.*, 2009, Figure 8]. In a similar way, the westward tilt of blobs on the two planes which are not coplanar (i.e., on the horizontal and perpendicular planes) suggests that the blob appears as a portion of a three-dimensional tilted shell structure, as shown in Figure 5.

For the example in Figure 1 the blob tilt angles on the horizontal plane (β) are −55° and −52° when Methods A and B are used, respectively. As was mentioned in section 3 and exemplified in Figure 2, the blob tilt angles on the perpendicular plane (α) are about −28° on average. Using the relationship between these two angles, we can check if the blob structure is field aligned. To simplify the problem, we assume that the blob structure is a slanted plane. A local Cartesian coordinate system is used in the following discussion; the x' direction is toward magnetic east (the same as the zonal direction in the MFA coordinate system, see section 2), the z'

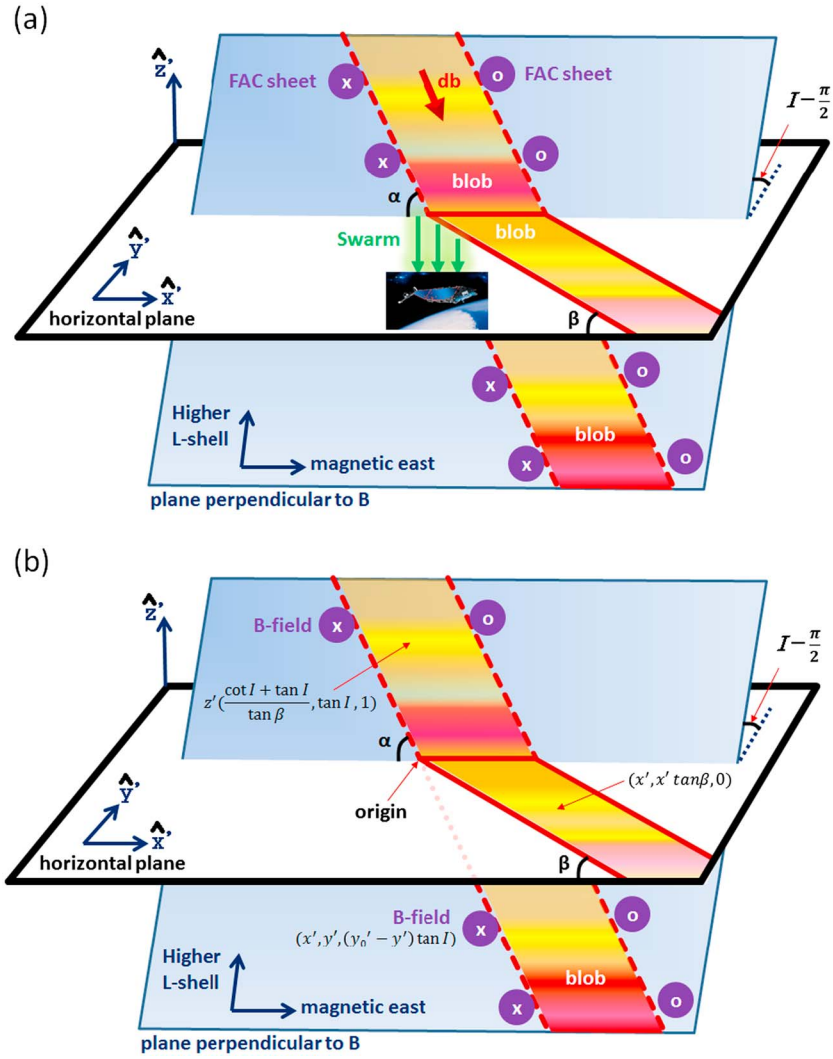

Figure 5. Three-dimensional perspective of blob structures on a local scale.

direction is directed vertically upward, and the y' direction completes the triad pointing toward magnetic north on the horizontal plane. For simplicity, we locally approximate the mean field lines by straight lines, and the location where Swarm encounters a blob is set to the origin. Then, each B field line should satisfy the following condition:

$$z' = (y'_0 - y')\ \tan I, \tag{1}$$

where y'_0 is the y' value when the B field line encounters the x'-y' plane, and the angle I is the inclination or dip angle of the geomagnetic field. Hence, the perpendicular plane containing the origin can be described by the following equation:

$$z' = y'\ \cot I. \tag{2}$$

In terms of the angle β (see Figure 5), the blob trace on the horizontal plane ($z' = 0$) has to satisfy the following equation:

$$y' = x'\ \tan\beta \quad \text{and} \quad z' = 0. \tag{3}$$

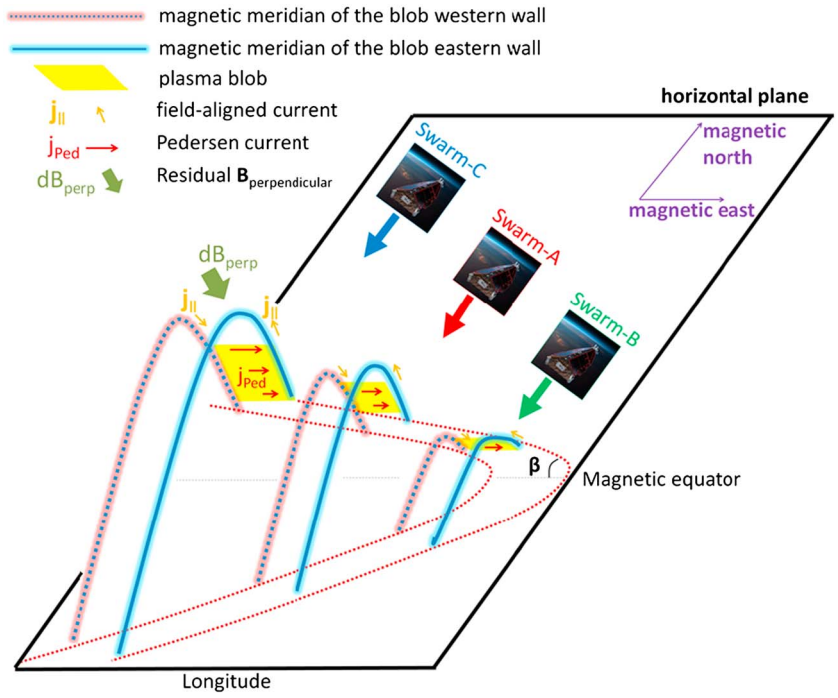

Figure 6. Three-dimensional perspective of blob structures on the global scale.

We assume that this linear trace (equation (3)) is extended along the mean field line: that is, we assume that the blob is field aligned. As we locally approximate the mean field lines by straight lines, the resultant blob structure should be a plane satisfying equations (1) and (3) simultaneously:

$$z' = (x' \tan\beta - y') \times \tan I. \tag{4}$$

The blob trace on the perpendicular plane should satisfy equations (2) and (4) simultaneously. From equation (2) y' can be expressed as a function of z':

$$y' = z' \tan I. \tag{5}$$

In a similar way, x' can be expressed as a function of z' from equations (4) and (5):

$$x' = \frac{z' \cot I + y'}{\tan\beta} = \frac{z' \cot I + z' \tan I}{\tan\beta} = z' \frac{\cot I + \tan I}{\tan\beta}. \tag{6}$$

Hence, the blob trace on the perpendicular plane can be expressed as

$$(x', y', z') = z' \left(\frac{\cot I + \tan I}{\tan\beta}, \tan I, 1 \right). \tag{7}$$

I in this equation, which is considered constant within a blob, can be given by geomagnetic field models or approximated as $I \approx 2 \times MLAT$. Note also that z' can be either positive or negative. From the inner product of equation (7) with $(x', y', z') = (1, 0, 0)$, we can estimate the angle between the magnetic east and the blob trace on the perpendicular plane (α: see Figure 5):

$$\alpha_{\text{calculated}} = \cos^{-1}\left(\pm \frac{\cot I + \tan I}{\tan\beta} \frac{1}{\sqrt{\left(\frac{\cot I + \tan I}{\tan\beta}\right)^2 + \tan^2 I + 1}} \right) \approx 145^\circ \text{ or } -35^\circ. \tag{8}$$

for the blobs shown in Figures 1 and 2.

This angle $\alpha_{calculated}$ (about −35°) qualitatively agrees with the observed tilt angles on the perpendicular plane, α, given in section 3 (about −28°). For the 14 blob events exhibiting westward tilt on the horizontal plane, the agreement between the calculated and observed α is quite good: the difference between the calculated and observed α is 3° ± 15° on average (see Table 1). Considering that a field-aligned blob structure was assumed in deriving equation (4), the *good* agreement between the calculated and observed α suggests "field-aligned" meridional cross sections of the blob shell structures: see Figure 6. This result is consistent with case studies of *Park et al.* [2008], which reported blob encounters by two or three conjugate satellites at different altitudes.

The shell structure of blobs tells us little about the mechanism of blob generation, i.e., whether blobs originate from EPBs or not. Even though EPBs and blobs may be generated independently, both can exhibit similar westward tilt (or shell structure) caused by the well-known latitudinal shear in zonal drift of background ionospheric plasma [e.g., *Kil et al.*, 2009, Figure 6]. Further studies are warranted to clarify the relationship between EPBs and blobs, which is still discussed controversy.

5. Summary

The early commissioning phase of the Swarm satellite constellation between December 2013 and mid-January 2014 provided a unique opportunity to clarify the three-dimensional structure of low-latitude plasma blobs. During the period we could identify 15 blob events which were encountered near simultaneously by all the three Swarm satellites. The 15 blob events exhibited the following properties:

1. Fourteen out of the 15 blobs exhibited a westward tilt on the 'horizontal' plane. For the remaining one event it was not easy to derive a reliable tilt direction: we suppose that the three Swarm satellites did not sample the same blob.
2. For all the 15 blobs zonal and meridional residual *B* fields exhibited an anticorrelation of their variations, with a median of the correlation coefficient of about −0.69. This result implies that FAC sheets related to the blobs are tilted westward on the 'perpendicular' plane (i.e., on the plane perpendicular to the ambient *B* field).
3. The relationship between the tilt angles on the horizontal and perpendicular planes supports that the meridional cut of the blob structure is field aligned.
4. Combining the three results mentioned above, we conclude that blobs observed during this period are generally contained within tilted shells of geomagnetic flux tubes, which are similar to the EPB shell structure suggested and confirmed previously [e.g., *Kil et al.*, 2009; *Park et al.*, 2009].

Acknowledgments
We sincerely thank C. Xiong and H. Kil for helpful discussions. The official Swarm website is http://earth.esa.int/swarm. The server for Swarm data distribution is ftp://swarm-diss.eo.esa.int. The Swarm data have been provided to GFZ under the ESA/ESTEC contract 4000102140/10/NL/JA. J. Park was partially supported by the "Planetary system research for space exploration" project, the basic research funding from KASI, and the Air Force Research Laboratory, under agreement FA2386-14-1-4004.

Alan Rodger thanks the reviewers for their assistance in evaluating this paper.

References

Aggson, T. L., W. J. Burke, N. C. Maynard, W. B. Hanson, P. C. Anderson, J. A. Slavin, W. R. Hoegy, and J. L. Saba (1992), Equatorial bubbles updrafting at supersonic speeds, *J. Geophys. Res.*, *97*(A6), 8581–8590, doi:10.1029/92JA00644.

Choi, H.-S., H. Kil, Y.-S. Kwak, Y.-D. Park, and K.-S. Cho (2012), Comparison of the bubble and blob distributions during the solar minimum, *J. Geophys. Res.*, *117*, A04314, doi:10.1029/2011JA017292.

Haaser, R. A., G. D. Earle, R. A. Heelis, J. Klenzing, R. Stoneback, W. R. Coley, and A. G. Burrell (2012), Characteristics of low-latitude ionospheric depletions and enhancements during solar minimum, *J. Geophys. Res.*, *117*, A10305, doi:10.1029/2012JA017814.

Huang, C.-S., G. Le, O. de La Beaujardière, P. A. Roddy, D. E. Hunton, R. F. Pfaff, and M. R. Hairston (2014), Relationship between plasma bubbles and density enhancements: Observations and interpretation, *J. Geophys. Res. Space Physics*, *119*, 1325–1336, doi:10.1002/2013JA019579.

Kelley, M. C., J. J. Makela, L. J. Paxton, F. Kamalabadi, J. M. Comberiate, and H. Kil (2003), The first coordinated ground- and space-based optical observations of equatorial plasma bubbles, *Geophys. Res. Lett.*, *30*(14), 1766, doi:10.1029/2003GL017301.

Kil, H., R. A. Heelis, L. J. Paxton, and S. J. Oh (2009), Formation of a plasma depletion shell in the equatorial ionosphere, *J. Geophys. Res.*, *114*, A11302, doi:10.1029/2009JA014369.

Kil, H., H.-S. Choi, R. A. Heelis, L. J. Paxton, W. R. Coley, and E. S. Miller (2011), Onset conditions of bubbles and blobs: A case study on 2 March 2009, *Geophys. Res. Lett.*, *38*, L06101, doi:10.1029/2011GL046885.

Klenzing, J. H., D. E. Rowland, R. F. Pfaff, G. Le, H. Freudenreich, R. A. Haaser, A. G. Burrell, R. A. Stoneback, W. R. Coley, and R. A. Heelis (2011), Observations of low-latitude plasma density enhancements and their associated plasma drifts, *J. Geophys. Res.*, *116*, A09324, doi:10.1029/2011JA016711.

Le, G., C.-S. Huang, R. F. Pfaff, S.-Y. Su, H.-C. Yeh, R. A. Heelis, F. J. Rich, and M. Hairston (2003), Plasma density enhancements associated with equatorial spread F: ROCSAT-1 and DMSP observations, *J. Geophys. Res.*, *108*(A8), 1318, doi:10.1029/2002JA009592.

Martinis, C., J. Baumgardner, M. Mendillo, S.-Y. Su, and N. Aponte (2009), Brightening of 630.0 nm equatorial spread-F airglow depletions, *J. Geophys. Res.*, *114*, A06318, doi:10.1029/2008JA013931.

Miller, E. S., H. Kil, J. J. Makela, R. A. Heelis, E. R. Talaat, and A. Gross (2014), Topside signature of medium-scale traveling ionospheric disturbances, *Ann. Geophys.*, *32*, 959–965, doi:10.5194/angeo-32-959-2014.

Oya, H., T. Takahashi, and S. Watanabe (1986), Observation of low latitude ionosphere by the impedance probe on board the Hinotori satellite, *J. Geomagn. Geoelec.*, *38*, 111–123.

Park, J., K. W. Min, J.-J. Lee, H. Kil, V. P. Kim, H.-J. Kim, E. Lee, and D. Y. Lee (2003), Plasma blob events observed by KOMPSAT-1 and DMSP F15 in the low latitude nighttime upper ionosphere, *Geophys. Res. Lett.*, *30*(21), 2114, doi:10.1029/2003GL018249.

Park, J., C. Stolle, H. Lühr, M. Rother, S.-Y. Su, K. W. Min, and J.-J. Lee (2008), Magnetic signatures and conjugate features of low-latitude plasma blobs as observed by the CHAMP satellite, *J. Geophys. Res.*, *113*, A09313, doi:10.1029/2008JA013211.

Park, J., H. Lühr, C. Stolle, M. Rother, K. W. Min, and I. Michaelis (2009), The characteristics of field-aligned currents associated with equatorial plasma bubbles as observed by the CHAMP satellite, *Ann. Geophys.*, *27*, 2685–2697.

Park, J., H. Lühr, C. Stolle, M. Rother, K. W. Min, and I. Michaelis (2010), Field-aligned current associated with low-latitude plasma blobs as observed by the CHAMP satellite, *Ann. Geophys.*, *28*, 697–703, doi:10.5194/angeo-28-697-2010.

Pimenta, A. A., Y. Sahai, J. A. Bittencourt, M. A. Abdu, H. Takahashi, and M. J. Taylor (2004), Plasma blobs observed by ground-based optical and radio techniques in the Brazilian tropical sector, *Geophys. Res. Lett.*, *31*, L12810, doi:10.1029/2004GL020233.

Stolle, C., H. Lühr, M. Rother, and G. Balasis (2006), Magnetic signatures of equatorial spread F, as observed by the CHAMP satellite, *J. Geophys. Res.*, *111*, A02304, doi:10.1029/2005JA011184.

Watanabe, S., and H. Oya (1986), Occurrence characteristics of low latitude ionospheric irregularities observed by impedance probe on board Hinotori satellite, *J. Geomagn. Geoelec.*, *38*, 125–149.

Woodman, R. F. (2009), Spread F—An old equatorial aeronomy problem finally resolved, *Ann. Geophys.*, *27*, 1915–1934, doi:10.5194/angeo-27-1915-2009.

Yokoyama, T., S.-Y. Su, and S. Fukao (2007), Plasma blobs and irregularities concurrently observed by ROCSAT-1 and equatorial atmosphere radar, *J. Geophys. Res.*, *112*, A05311, doi:10.1029/2006JA012044.